Proceedings of the Symposium A of the European Materials Research, Warsaw, September 2008

Low-Frequency Raman Scattering from ZnO(Fe) Nanoparticles

R. Kostić[a], N. Romčević[a,*], M. Romčević[a], B. Hadžić[a], R. Rudolf[b,c], I. Kuryliszyn-Kudelska[d], W. Dobrowolski[d], U. Narkiewicz[e] and D. Sibera[e]

[a]Institute of Physics, Pregrevica 118, 11080 Belgrade, Serbia

[b]Faculty of Mechanical Engineering, University of Maribor, Smetanova 17, 2000 Maribor, Slovenia

[c]Zlatarna Celje d.d., Kresnikova 19, 3000 Celje, Slovenia

[d]Institute of Physics, Polish Academy of Sciences, al. Lotników 32/46, 02-668 Warszawa, Poland

[e]Szczecin University of Technology, Institute of Chemical and Environment Engineering Pułaskiego 10, 70-322 Szczecin, Poland

Nanocrystalline samples of ZnO(Fe) were synthesized by wet chemical method. Samples were characterized by X-ray diffraction to determine the sample composition and the mean crystalline size. Low-frequency Raman modes were measured and assigned according to confined acoustic vibrations of spherical nanoparticles. Frequencies of these vibrational modes were analyzed in elastic continuum aproximation, which considers nanoparticle as homogeneous elastic sphere.

PACS numbers: 78.30.Fs, 78.67.−n

1. Introduction

Nanostructures made of ZnO have attracted significant attention owing to their proposed applications in low-voltage and short-wavelength electro-optical devices, transparent ultraviolet protection films, and spintronic devices [1, 2]. A considerable attention has recently been devoted to high temperature ferromagnetism observed in transition metal doped oxides. Particularly ZnO has been identified as a promising host semiconductor material, exhibiting ferromagnetism when doped with most of the transition metals — V, Cr, Fe, Co, Ni [3]. However, the origin of ferromagnetic behavior is not very well known in these compounds. Recently, it was shown that the ferromagnetism in these materials can be induced by inclusions of nanoscale oxides of transition metals [4] and/or nanoparticles containing a large concentration of magnetic ions [5]. Novel methods enabling a control of nanoassembling of magnetic nanocrystals in nonconducting matrices as well as functionalities specific to such systems were described [5].

The samples were synthesized by use of the wet chemical method. First, the mixture of iron and zinc hydroxides was obtained by addition of an ammonia solution to the 20% solution of proper amount of $Zn(NO_3)\cdot 6H_2O$ and $Fe(NO_3)\cdot 4H_2O$ in water. Next, the obtained hydroxides were filtered, dried and calcined at 300°C during one hour. A series of samples containing from 5 to 95% of Fe_2O_3 was obtained. The phase composition of the samples was determined by X-ray diffraction (XRD) (Co K_α radiation, X'Pert Philips). The crystalline phases of hexagonal ZnO, rhombohedric Fe_2O_3 and cubic $ZnFe_2O_4$ were identified as presented in [6].

XRD data allowed us to determine a mean crystallite size in prepared samples by use of Scherrer's formula. The mean crystalline size a of these phases are given in Table I in Ref. [6].

In this work we present investigation of two samples. First sample is assigned as $(ZnO)_{0.95}(Fe_2O_3)_{0.05}$ (sample contains 5 wt.% of Fe_2O_3), where crystalline phase of $ZnFe_2O_4$ is identified. Mean crystallite size is $a = 10$ nm. Second sample is assigned as DS90Fe10Zn (sample contains 90 wt.% of Fe_2O_3) where crystallite of Fe_2O_3 is identified with mean crystallite size $a = 24$ nm. No other crystal phases are observed in these samples.

XRD measurements did not reveal presence of ZnO phase in these samples. It is interesting that for the samples with lower concentration of Fe_2O_3 (up to 20 wt.% of Fe_2O_3) excitonic lines from ZnO are observed. In some samples, for instance sample containing 40 wt.% of Fe_2O_3, crystallites of ZnO and $ZnFe_2O_4$ are identified [6].

2. Results and discussion

The Raman spectra were excited by the 514.5 nm line of an Ar laser (the average power was about 120 mW) in the backscattering geometry. We used Jobin Yvon model U-1000 monochromator, with a conventional photocounting system. In order to make low-frequency Raman modes visible we subtracted the intensity of the elastic scattering background by A/ω^n approximation. Re-

* corresponding author; e-mail: romcevi@phy.bg.ac.yu

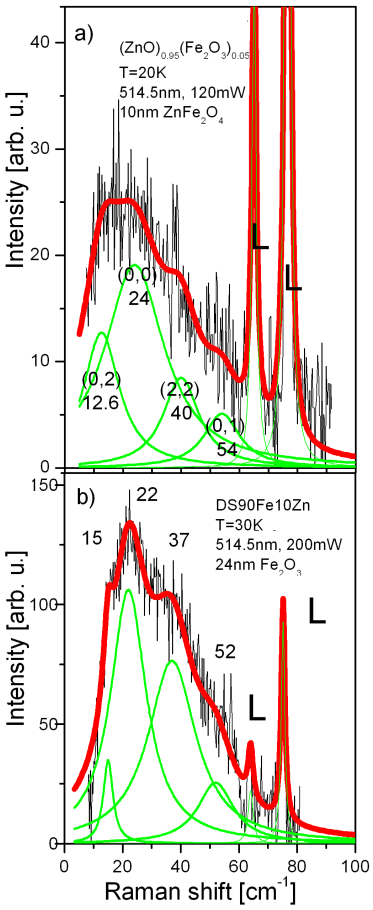

Fig. 1. Low-frequency Raman spectra of sample: (a) $(ZnO)_{0.95}(Fe_2O_3)_{0.05}$ where $ZnFe_2O_4$ crystallites of $a = 10$ nm size are identified, (b) DS90Fe10Zn where Fe_2O_3 crystallites of $a = 24$ nm size are identified.

sulting Raman spectra are presented in Fig. 1. The observed modes are deconvoluted using the Lorentzian line profile technique. For almost all samples, low-frequency Raman modes were identified.

Low-frequency modes are analyzed as confined acoustic vibrations of nanoparticles. The frequencies of acoustic vibrational modes can be calculated in the elastic continuum approximation. Parameters of the model are stiffness constants and mass density of the particle material. In doped samples $ZnFe_2O_4$ and Fe_2O_3 structures are identified. As the dimension of the particles is already determined and having in mind specific frequency to diameter dependence, we established material parameters and analyzed behavior of nanoparticles.

Transverse (v_T) and longitudinal (v_L) sound velocity are parameters of equation of motion of the three-dimensional elastic body. Transverse and longitudinal sound velocity are directly connected to stiffness constants and the mass density. If we assume that nanoparticles are small spheres, equation of motion must be solved in spherical coordinate. It is useful to introduce dimensionless variables $\eta = \omega R/v_T = \omega d/2v_T$ and $\xi = \omega R/v_L = \omega d/2v_L$, where R is radius of the particle (d is diameter). Boundary conditions definitely determine the solutions [7–11].

If one assumes that there is no displacement at the particle surface, it is so-called rigid boundary conditions. If one assumes that there is no force on the surface, i.e. radial components of the stress tensor at the surface are zero, it is so-called free-surface boundary conditions. We assumed the stress-free boundary conditions [10]. We believe that this model is adequate to describe behavior of nanoparticles in our samples, as there is no compact matrix surrounding them.

In spherical case, each value of angular momentum quantum number l ($l = 0, 1, 2, \ldots$) gives a series of solutions. We numerate these solutions n ($n = 0, 1, 2, \ldots$). So, eigensolutions are labeled as η^{nl} (ξ^{nl}), and eigenstates are labeled as (n, l). Two types of vibrational modes are obtained: spheroidal and torsional modes. As $\omega^{nl} = 2\eta^{nl}v_T/d$, i.e. $\omega^{nl} = 2\xi^{nl}v_L/d$, each solution gives one linear dependence $\omega^{nl} = f(1/d)$.

Dimensionless solutions of equation for spheroidal modes strongly depend on the material through ratio v_L/v_T. Solutions for torsional modes do not depend on material. According to the group theory analysis the spheroidal and $l = 0$ and $l = 2$ modes are Raman active [12]. Theory implies [13] that the spheroidal mode (0, 0) is the most intensive in the $l = 0$ series, and is the most intensive of all Raman active modes. In a lot of experimental spectra only this mode was detected. The first quadrupolar mode is the most intensive in $l = 2$ series. The frequency of (0, 2) mode is almost always lower than the (0, 0) mode frequency.

Structure of $ZnFe_2O_4$ is similar to Fe_3O_4. In our analysis we started from Fe_3O_4 acoustic properties. For Fe_3O_4 of spinel (cubic) structure we used following parameters: mass density 5240 kg/m^3 and stiffness constants $C_{11} = 2.17 \times 10^{11}$ N/m^2, $C_{12} = 1.21 \times 10^{11}$ N/m^2, $C_{44} = 0.46 \times 10^{11}$ N/m^2 [14]. Longitudinal and transverse sound velocities in a case of cubic crystal are: $v_L = (C_{11}/\rho)^{1/2} = 6400$ m/s and $v_T = (C_{44}/\rho)^{1/2} = 2960$ m/s. Solutions for Fe_3O_4, in case of stress-free boundary conditions, for the $l = 0$, $n = 0$, 1, 2 and $l = 2$, $n = 0$, 1, 2, 3, 4 are presented in Fig. 2a. We marked (solid cycles) positions of frequencies that are a result of deconvolution of $ZnFe_2O_4$ particles experimental spectra. First two frequencies, that are the best defined structures in spectra, are located very close to Fe_3O_4 (0, 0) and (0, 2) solutions, Fig. 2a. Also the mode at ≈ 24 cm^{-1} is more intensive than the mode at ≈ 12.6 cm^{-1}.

We tentatively attributed mode at 24 cm^{-1} to be ω^{00} (0, 0) and mode at 12.6 cm^{-1} to be ω^{02} (0, 2). As $\omega^{00} = 2\xi^{00}v_L/d$ and $\omega^{02} = 2\eta^{02}v_T/d = 2\xi^{02}v_L/d$ follows that $\omega^{00}/\omega^{02} = \xi^{00}/\xi^{02} = 1.9$. From curves $\xi^{00}(v_L/v_T)$ and $\xi^{02}(v_L/v_T)$ function $g(v_L/v_T) = \xi^{00}(v_L/v_T)/\xi^{02}(v_L/v_T)$ can be established. As $\omega^{00}/\omega^{02} = 1.9$, from $g(v_L/v_T)$ follows that $v_L/v_T = 1.9$ and $\xi^{00}(1.9) = 2.68$. ¿From $\omega^{00} = 24$ cm^{-1}, $d = 10$ nm follows: $v_L = 8355$ m/s and $v_T = v_L/1.9 = 4397$ m/s. These are new parameters

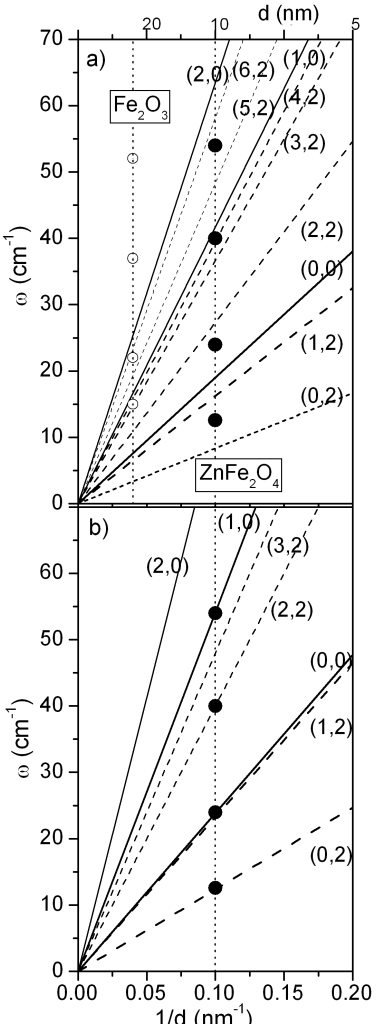

Fig. 2. (a) Dependence of eigensolutions, for spheroidal modes in the surface stress-free approximation, on Fe_3O_4 nanoparticles inverse diameter: $v_L = 6400$ m/s and $v_T = 2960$ m/s. Plotted lines represent eigensolutions. Solid and open circles are experimental results of $ZnFe_2O_4$ and Fe_2O_3, respectively. (b) Dependence of eigensolutions on nanoparticles inverse diameter: $v_L = 8355$ m/s and $v_T = 4397$ m/s. Solid circles are experimental results of $ZnFe_2O_4$.

that can be prescribed to $ZnFe_2O_4$. We solved complete problem with these new parameters. New solutions are presented in Fig. 2b.

Basic assumption was that $\omega^{00} = 24$ cm^{-1} and $\omega^{02} = 12.6$ cm^{-1}. As we see $\omega^{12} \approx \omega^{00}$ and cannot be separated and detected in experimental spectra. Band at ≈ 40 cm^{-1} is identified as (2, 2) and band at ≈ 54 cm^{-1} as (1, 0) mode. Very good agreement between experimental and calculated results imply that our assumptions were correct.

In Fig. 2a we marked (open cycles) frequency positions that are a result of experimental Fe_2O_3 particles spectra deconvolution ($d = 24$ nm). As expected experimental frequencies are far away from calculated Fe_3O_4 values. For cubic system it is reasonable to use effective i.e. averaged parameters, as we did for Fe_3O_4 and $ZnFe_2O_4$. α-Fe_2O_3 crystallize in rhombohedric (trigonal) system, conventionally viewed as hexagonal. Stiffness constants, and consequently sound velocities, differ very much for different crystallographic axes in α-Fe_2O_3 and from Fe_3O_4 values. It was not reasonable to follow the procedure with averaged parameters as in $ZnFe_2O_4$. For investigation of low-frequency Raman spectra of Fe_2O_3 more detailed analysis is needed.

3. Conclusion

In this work we present low-frequency Raman spectra of $ZnFe_2O_4$ nanoparticles. We found that the observed peaks agree well with the calculated frequencies of acoustic phonons. As a result we identified (0, 2), (0, 0), (2, 2) and (1, 0) modes.

Acknowledgments

This work was supported under the Agreement of Scientific Collaboration between Polish Academy of Sciences and Serbian Academy of Sciences and Arts. The work in Serbia was supported by Serbian Ministry of Science (projects No. 141028 and No. 141047) and OPSA-026283 project within the EC FP6 programme.

References

[1] Y. Chen, D.M. Bagnall, H. Koh, K. Park, K. Higara, Z. Zhu, T. Yao, *J. Appl. Phys.* **84**, 3912 (1988).

[2] J. Nemeth, G. Rodriguez-Gattorno, A. Diaz, I. Dekany, *Langmuir* **20**, 2855 (2004).

[3] J.M.D. Coey, M. Venkatesan, C.B. Fitzgerald, *Nature Mater.* **4**, 173 (2005).

[4] C. Sudakar, J.S. Thakur, G. Lawes, R. Naik, V.M. Naik, *Phys. Rev. B* **75**, 054423 (2007).

[5] T. Dietl, *Acta Phys. Pol. A* **111**, 27 (2007).

[6] U. Narkiewicz, D. Sibera, I. Kuryliszyn-Kudelska, L. Kilanski, W. Dobrowolski, N. Romcevic, *Acta Phys. Pol. A* **113**, 1695 (2008).

[7] A. Tanaka, S. Onari, T. Arai, *Phys. Rev. B* **47**, 1237 (1993).

[8] L. Saviot, B. Champagnon, E. Duval, A.I. Ekimov, *Phys. Rev. B* **57**, 341 (1998).

[9] L. Saviot, D.B. Murray, M. del C. Marco de Lucas, *Phys. Rev. B* **69**, 113402 (2004).

[10] L. Saviot, B. Champagnon, E. Duval, I.A. Kudriavtsev, I.E. Akimov, *J. Non-Cryst. Solids* **197**, 238 (1996).

[11] E. Roca, C. Trallero-Giner, M. Cardona, *Phys. Rev. B* **49**, 13704 (1994).

[12] E. Duval, *Phys. Rev. B* **46**, 5795 (1992).

[13] N. Combe, J.R. Huntzinger, A. Mlayah, *Phys. Rev. B* **76**, 205425 (2007).

[14] P. Nordlander, M. Ronay, *Phys. Rev. B* **36**, 4982 (1987).